JPE 8-1-8

Battery Energy Storage System Based Controller for a Wind Turbine Driven Isolated Asynchronous Generator

Bhim Singh† and Gaurav Kumar Kasal*

†*Dept. of Electrical Eng., Indian Institute of Technology, New Delhi, India

ABSTRACT

This paper presents an investigation of a voltage and frequency controller for an isolated asynchronous generator (IAG) driven by a wind turbine and supplying 3-phase 4-wire loads to the isolated areas where a grid is not accessible. The control strategy is based on the indirect current control of the VSC (voltage source converter) using the frequency PI controller. The proposed controller consists of three single-phase IGBT (Insulated Gate Bipolar Junction Transistor) based VSC, which are connected to each phase of the IAG through three single phase transformers and a battery at their DC link. The controller has the capability of controlling reactive and active powers to regulate the magnitude and frequency of the generated voltage, harmonic elimination, load balancing and neutral current compensation. The proposed isolated system is modeled and simulated in MATLAB using Simulink and PSB (Power System Block-set) toolboxes to verify the performance of the controller.

Keywords: isolated asynchronous generator, wind turbine, voltage and frequency controller, 3-phase 4-wire system

1. Introduction

Isolated asynchronous generators (IAGs), which are also known as a self excited induction generators (SEIG), with their low maintenance and simplified control, appear to be an effective solution for isolated hydro and wind power applications [1-4] where grid supply is not accessible and where areas are rich in renewable energy sources. In pico hydro applications, there is a number of low cost schemes which are available to control the voltage and frequency of an IAG [5-8]. Substantial work has also been done to study the state and transient behavior of isolated [9-12], as well as grid connected [13-16], wind power applications along with regulating the magnitude and frequency of the system voltage. However, in a grid connected wind power application, the frequency remains constant due to the availability of the grid but is a greater challenge in an isolated mode of operation under the conditions of varying wind speeds. After a careful review of the literature [5-12] it is observed that previously reported work concentrated only on 3-phase 3-wire or single phase power applications of the IAG.

In this paper an effort is made to investigate a controller for the wind turbine driven IAG to feed 3-phase 4-wire loads in remote communities where grid supply is not accessible. An investigation of such a system is necessary because most of the loads in such communities are single

Manuscript received Aug. 31, 2007; revised Nov. 26, 2007
† Corresponding Author: gauravkasal@gmail.com
Tel: +91-9899496868, I.I.T., New Delhi, India
*Dept. of Electrical Eng., I.I.T., New Delhi, India

phase distributed loads. The proposed controller consists of three single-phase IGBT (Insulated Gate Bipolar Junction Transistor) based voltage source converter (VSC), which are connected to each phase of IAG through three single phase transformers [17] and a battery at its DC link [18]. In addition to controlling the magnitude and frequency of the generated voltage it also has the capability of harmonic elimination, load balancing, load leveling and neutral current compensation under any dynamic condition like variation of consumer load or speed of the wind. There is also an additional feature that the neutral point for the load is created through the neutral point of the capacitor bank and terminals of the single phase transformers which provides the choice to connect the machine either in star or delta configuration.

2. System Configuration and Principle of Operation

Fig 1 shows the schematic diagram of the proposed electro-mechanical system along-with its controller, excitation capacitor and consumer loads. A star connected excitation capacitor bank with neutral terminal 'n' is used to generate the rated voltage at no-load, while additional demand of excitation to regulate the voltage is met by the controller. The neutral point for the consumer loads is created through a neutral point of the excitation capacitor bank and the transformer of the proposed controller.

The proposed controller is realized using three single-phase IGBT based voltage source converters (VSCs) with a battery at its DC bus. Each phase of VSC is

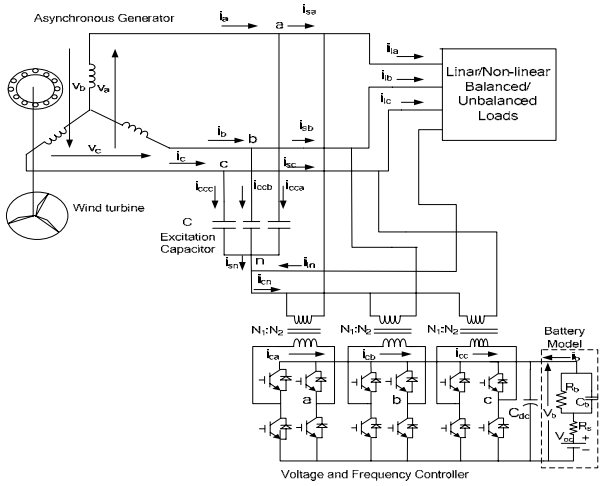

Fig. 1 Schematic diagram of VF controller for a IAG Driven wind turbine feeding 3-phase 4-wire loads

connected to the generator through three single-phase transformers. Advantages of using such 3-phase 4-wire topology of the VSC include voltage rating of the battery is selected at optimum level and the transformer provides the path for flowing neutral currents. The proposed controller is having a bi-directional flow capability of active and reactive powers by which it can control the magnitude and frequency of the generator voltage during different dynamic conditions like variation in consumer

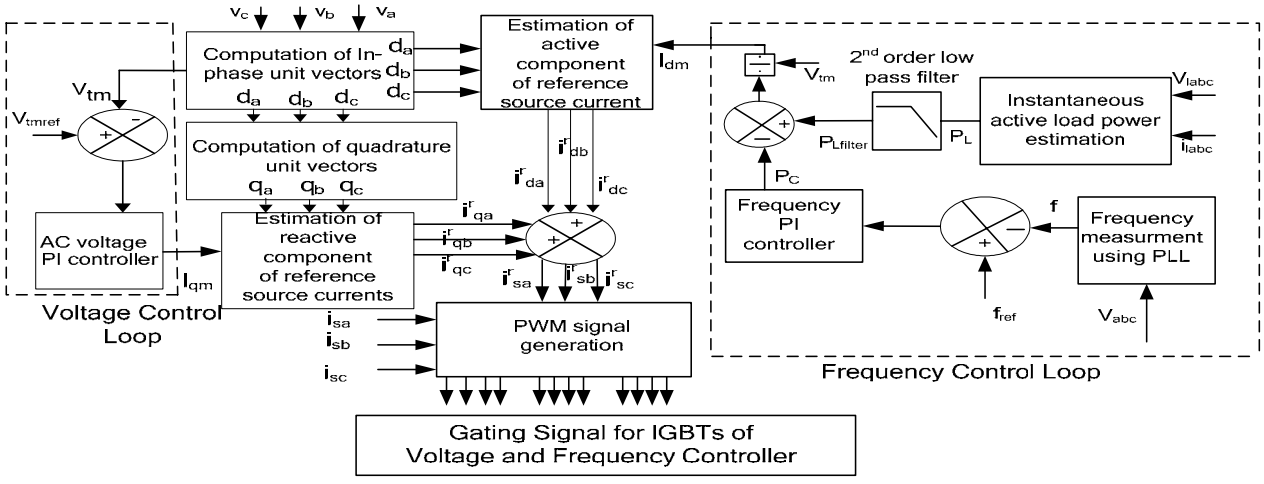

Fig. 2 Schematic diagram of control scheme for VF controller in 3-phase 4-wire application of wind turbine driven IAG

loads and under the condition of varying wind speeds.

For maintaining constant frequency, total generated power should be consumed by the applied load (consumer load + battery). Here a frequency controller is used for extracting the active component of the source current. When there is a deficiency in the generated power, the battery supplies the additional required load demand through a process of discharging, and maintains the constant frequency along with providing the functions of load leveling. While there is an excess of generated power, it starts charging the battery and consumes additional generated power which is not consumed by the consumer loads.

3. Control Scheme

As shown in Fig. 2 the control strategy of the proposed voltage and frequency controller is realized through derivation of reference source currents (i^r_{sa}, i^r_{sb}, i^r_{sc}). Three-phase reference source currents consist of two components; one is in phase or active component (i^r_{da}, $i^r_{db,}$ i^r_{dc}) for regulating the frequency, while other one is in quadrature or reactive component (i^r_{qa}, $i^r_{qb,}$ i^r_{qc}) for regulating the terminal voltage. The amplitude of the active power component of the source current (I_{dm}) is estimated by dividing the difference of filtered load power ($P_{Lfilter}$) and output of PI frequency controller (P_c) to the amplitude of the terminal voltage (V_{tm}). The multiplication of I_{dm} with in-phase unit amplitude templates (d_a, d_b and d_c) yields the in-phase component of reference source currents. These templates are three-phase sinusoidal functions, which are derived by dividing the AC voltages v_a, v_b and v_c by their amplitude V_{tm}. To generate the quadrature component of reference source currents, another set of sinusoidal quadrature unity amplitude templates (q_a, $q_{b,}$ q_c) is obtained from in-phase unit vectors (d_a, d_b and d_c). The multiplication of these components with output of the AC voltage PI controller (I_{qm}) gives the quadrature, or reactive component, of reference source currents. The sum of instantaneous quadrature and in-phase component of source currents is the reference source currents (i^r_{sa}, i^r_{sb} and i^r_{sc}), and each phase current is compared with the corresponding reference to generate the PWM unipolar switching signal for all three single-phase VSCs [19]. The unipolar switching scheme has the advantage of "effectively" doubling the ripple frequency as far as the output harmonics are concerned.

4. Control Algorithm

Basic equations of the control scheme of the proposed controller are as follows.

4.1 Computation of active component of reference source current

The active component of the reference source current is estimated by dividing the difference of filtered instantaneous load power ($P_{Lfilter}$) and output of the PI frequency controller to the terminal voltage (V_{tm}). The load power (P_L) is estimated as by taking the 3-phase to a 2-phase transformation:

$$v_\alpha = (\sqrt{2}/3)\,(v_{la} - ½\, v_{lb} - ½\, v_{lc}) \quad (1)$$

$$v_\beta = (\sqrt{2}/3)\,(\sqrt{3}/2\, v_{lb} - \sqrt{3}/2\, v_{lc}) \quad (2)$$

$$i_\alpha = (\sqrt{2}/3)\,(i_{la} - ½\, i_{lb} - ½\, i_{lc}) \quad (3)$$

$$i_\beta = (\sqrt{2}/3)\,(\sqrt{3}/2\, i_{lb} - \sqrt{3}/2\, i_{lc}) \quad (4)$$

Instantaneous active power is estimated as:

$$P_L = v_\alpha i_\alpha + v_\beta i_\beta \quad (5)$$

It is filtered to achieve its DC component ($P_{Lfilter}$).

The frequency error is defined as

$$f_{er(n)} = f_{ref(n)} - f_{(n)} \quad (6)$$

where f_{ref} is the reference frequency (50Hz in present system) and 'f' is the frequency of the voltage of an asynchronous generator. The instantaneous value of 'f' is estimated using the phase locked loop (PLL) at the terminals of the generator.

At the n^{th} sampling instant the output of frequency PI controller (P_c) is as:

$$P_{c(n)} = P_{c(n-1)} + K_{pf}\,\{ f_{er(n)} - f_{er(n-1)}\} + K_{if}\, f_{er(n)} \quad (7)$$

Then the active component of the reference source current (I_{dm}) is calculated as:

$$I_{dm} = 2(P_{Lfilter} - P_c)/ (3V_{tm}) \quad (8)$$

The instantaneous line voltages at the terminals of an asynchronous generator (v_a, v_b and v_c) are considered sinusoidal and their amplitude is computed as:

$$V_{tm} = \{(2/3) (v_a^2 + v_b^2 + v_c^2)\}^{1/2} \quad (9)$$

The unity amplitude templates are having instantaneous value in phase with instantaneous voltage (v_a, v_b and v_c), which are derived as

$$d_a = v_a/V_{tm} ; d_b = v_b/V_{tm} ; d_c = v_c/V_{tm} \quad (10)$$

Instantaneous values of in-phase components of reference source currents are estimated as:

$$i^r_{da} = I_{dm}\, d_a; \qquad i^r_{db} = I_{dm}\, d_b; i^r_{dc} = I_{dm}\, d_c; \quad (11)$$

4.2 Computation of reactive component of reference source current

The AC voltage error V_{er} at the n^{th} sampling instant is as

$$V_{er(n)} = V_{tmref(n)} - V_{tm(n)} \quad (12)$$

where $V_{tmref(n)}$ is the amplitude of the reference AC terminal voltage and $V_{tm(n)}$ is the amplitude of the sensed three-phase AC voltage at the terminals of an asynchronous generator at the n^{th} instant computed in eq (9)

The output of the PI controller ($I_{qm(n)}$) for maintaining constant AC terminal voltage at the n^{th} sampling instant is expressed as

$$I_{qm(n)} = I_{qm(n-1)} + K_{pa} \{ V_{er(n)} - V_{er(n-1)}\} + K_{ia} V_{er(n)} \quad (13)$$

where K_{pa} and K_{ia} are the proportional and integral gain constants of the proportional integral (PI) controller (values are given in Appendix). $V_{er\,(n)}$ and $V_{er(n-1)}$ are the voltage errors in n^{th} and $(n-1)^{th}$ instant and $I_{qm(n-1)}$ is the amplitude of the quadrature component of the reference source current at the $(n-1)^{th}$ instant.

The instantaneous quadrature components of reference source currents are estimated as

$$i^r_{qa} = I_{qm}\, q_a; i^r_{qb} = I_{qm}\, q_b; i^r_{qc} = I_{qm}\, q_c \quad (14)$$

where q_a, q_b and q_c are another set of unit vectors having a phase shift of 90º leading the corresponding unit vectors d_a, d_b and d_c which are computed as follows

$$q_a = -d_b / \sqrt{3} + d_c / \sqrt{3} \quad (15)$$
$$q_b = \sqrt{3}\, d_a / 2 + (d_b - d_c) / 2\sqrt{3} \quad (16)$$
$$q_c = -\sqrt{3}\, d_a / 2 + (d_b - d_c) / 2\sqrt{3} \quad (17)$$

4.3 Computation of reference source current

Total reference source currents are the sum of in-phase and quadrature components of the reference source currents as

$$i^r_{sa} = i^r_{qa} + i^r_{da} \quad (18)$$
$$i^r_{sb} = i^r_{qb} + i^r_{db} \quad (19)$$
$$i^r_{sc} = i^r_{qc} + i^r_{dc} \quad (20)$$

4.4 PWM signal generation

Reference source currents (i^r_{sa}, i^r_{sb} and i^r_{sc}) are compared with sensed source currents (i_{sa}, i_{sb} and i_{sc}). The current errors are computed as

$$i_{saerr} = i^r_{sa} - i_{sa} \quad (21)$$
$$i_{sberr} = i^r_{sb} - i_{sb} \quad (22)$$
$$i_{scerr} = i^r_{sc} - i_{sc} \quad (23)$$

These current errors are amplified using proportional controller by gain 'K' and which are as follows.

$$V_{cca} = K^* i_{saerr} \quad (24)$$
$$V_{ccb} = K^* i_{sberr} \quad (25)$$
$$V_{ccc} = K^* i_{scerr} \quad (26)$$

These amplified signals are compared with fixed frequency (10 kHz) triangular carrier wave to generate a unipolar PWM switching signal [19] to generate the gating signal for the VSC of each phase. For switching on the single phase VSC to the phase 'A', the basic logic is as:

$$\begin{Bmatrix} V_{cca} > V_{tri} & \text{(upper device of the left leg of phase 'A' on)} \\ V_{cca} < V_{tri} & \text{(lower device of the left leg of phase 'A' on)} \end{Bmatrix} \quad (27)$$

$$\begin{Bmatrix} -V_{cca} > V_{tri} & \text{(upper device of the right leg of phase 'A' on)} \\ -V_{cca} < V_{tri} & \text{(lower device of the right leg of phase 'A' on)} \end{Bmatrix} \quad (28)$$

where V_{tri} is taken as the amplitude of the fixed frequency

triangular wave and similar logic is applied to generate the gating signals for the two other phases.

5. MATLAB Based Modelling

Modeling of the proposed system including an asynchronous generator, a wind turbine and its controller, is carried out in MATLAB version of 7.1 using Simulink and PSB toolboxes. A brief description of each component is given as follows.

5.1 Modeling of mechanical system

The aerodynamic power generated by the wind turbine can be expressed as [20, 21]

$$P = 0.5\ \rho A C_p \upsilon_w^{\ 3} \tag{29}$$

where the aerodynamic power is expressed as a function of the specific density (ρ) of the air, the swept area of the blades (A) and the wind speed (υ_w).

To generate the constant frequency, the additional generated power with increased wind speed is stored into the battery and the speed of the generator is maintained at almost constant. Fig. 3 shows the curve between power coefficient (C_p) and tip speed ratio (λ) at the fixed degree pitch angle (β). It shows that C_p reaches a maximum value (0.48) for a maximum tip speed ratio (8.1), which yields the maximum mechanical power available in the wind turbine for a given wind speed. The tip speed ratio (TSR) is defined as the ratio of the linear speed at the tip of the blade ($\omega_T R$) and the wind speed (v_w), ω_T being the rotational speed of the wind turbine. The polynomial relation between C_p and λ at a particular pitch angle for considered wind turbine [20, 21] is represented as

$$C_p = C_1\ \{(C_2/\lambda i)-C_3\ \beta-C_4\}\}\ e^{-(C_5/\lambda i)} + C_6\lambda \tag{30}$$

where $1/\lambda i = \{1/(\lambda+C_7\ \beta)\} - \{C_8/(\beta^3+1)\}$ and $\beta = 0°$

5.2 Modeling of electrical system

The electrical system consists of an asynchronous generator with the excitation capacitor. An available model of an asynchronous machine including the saturation characteristics, which is determined by conducting a synchronous speed test on the machine, is considered into the model of the isolated generator. A bank of fixed value star connected excitation capacitor bank with neutral terminal 'n' is selected to generate the rated voltage at no-load while an additional demand of reactive power is met by the controller.

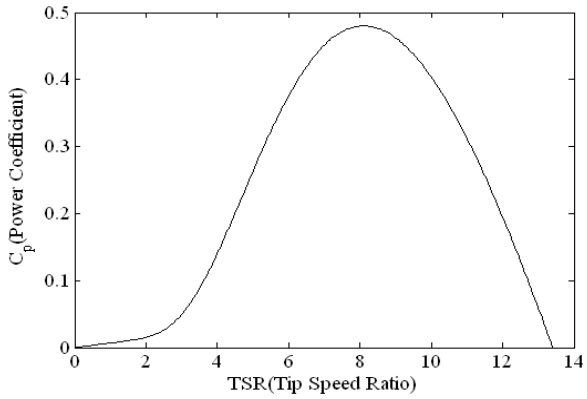

Fig. 3 Curve between power coefficients (C_p) and tip speed ratio (λ)

5.3 Modeling of the controller

The proposed voltage and frequency controller consists of CC-VSC (current controlled voltage source converter) with the battery at its DC link. In Fig 1, Thevenin's equivalent circuit of the battery based model is shown at the DC link of the controller. The terminal voltage of the equivalent battery (V_b) is obtained as follows

$$V_b > (N_2/N_1)\ (\sqrt{2}/\sqrt{3})\ V_l \tag{31}$$

where V_l is the line to line rms voltage of the generator and N_2/N_1 is turn ratio of transformer.

Since the battery is an energy storage unit, its energy is represented in kWh when a capacitor is used to model the battery unit, the capacitance can be determined from

$$C_b = \frac{kWh * 3600 * 10^3}{0.5(V_{ocmax}^{\ 2} - V_{ocmin}^{\ 2})} \tag{32}$$

In the Thevenin's equivalent model of the battery where R_s is the equivalent resistance (external + internal) of a parallel parallel/series combination of a battery, which is usually a small value. The parallel circuit of R_b and C_b is

used to describe the stored energy and voltage during charging or discharging. R_b in parallel with C_b, represents self discharging of the battery, since the self discharging current of a battery is small, the resistance R_b is large. Here the battery is considered of having 18 kW for 8 Hrs peaking capacity, and with the variation in the voltage of order of 440V-460V.

5.4 Modeling of the Consumer Loads

Linear and non-linear loads are modeled using available resistive and reactive elements and three single phase diode rectifier and L-C filter with resistive elements at it DC bus respectively in the PSB toolboxes of MATLAB.

6. Results and discussion

The performance of the proposed controller is demonstrated under different electrical and mechanical dynamic conditions. Figs 4 and 5 show the performance of the controller for supplying balanced/ unbalanced, linear/ non-linear loads. Fig. 6 demonstrates the performance of the controller under the condition of varying wind speeds and it is observed that in all conditions, the controller responds in a desired manner. Simulated transient waveforms of the generator voltage (v_{abc}), generator current(i_{abc}), capacitor current (i_{cca}), load currents (i_{labc}), controller current (i_{cabc}), neutral current of source (i_{sn}) load (i_{ln}) and compensator (i_{cn}), terminal voltage (v_{tm}), frequency (f), speed of the wind (v_w), battery current (i_b), battery voltage (v_b) and instantaneous active load power and filtered power (P_L and $P_{Lfilter}$), variation in power of battery (P_{bat}), consumer load (P_{load}) and generator (P_{gen}) are given under different dynamic (variation of consumer load and variation of wind speed) conditions. Table 1

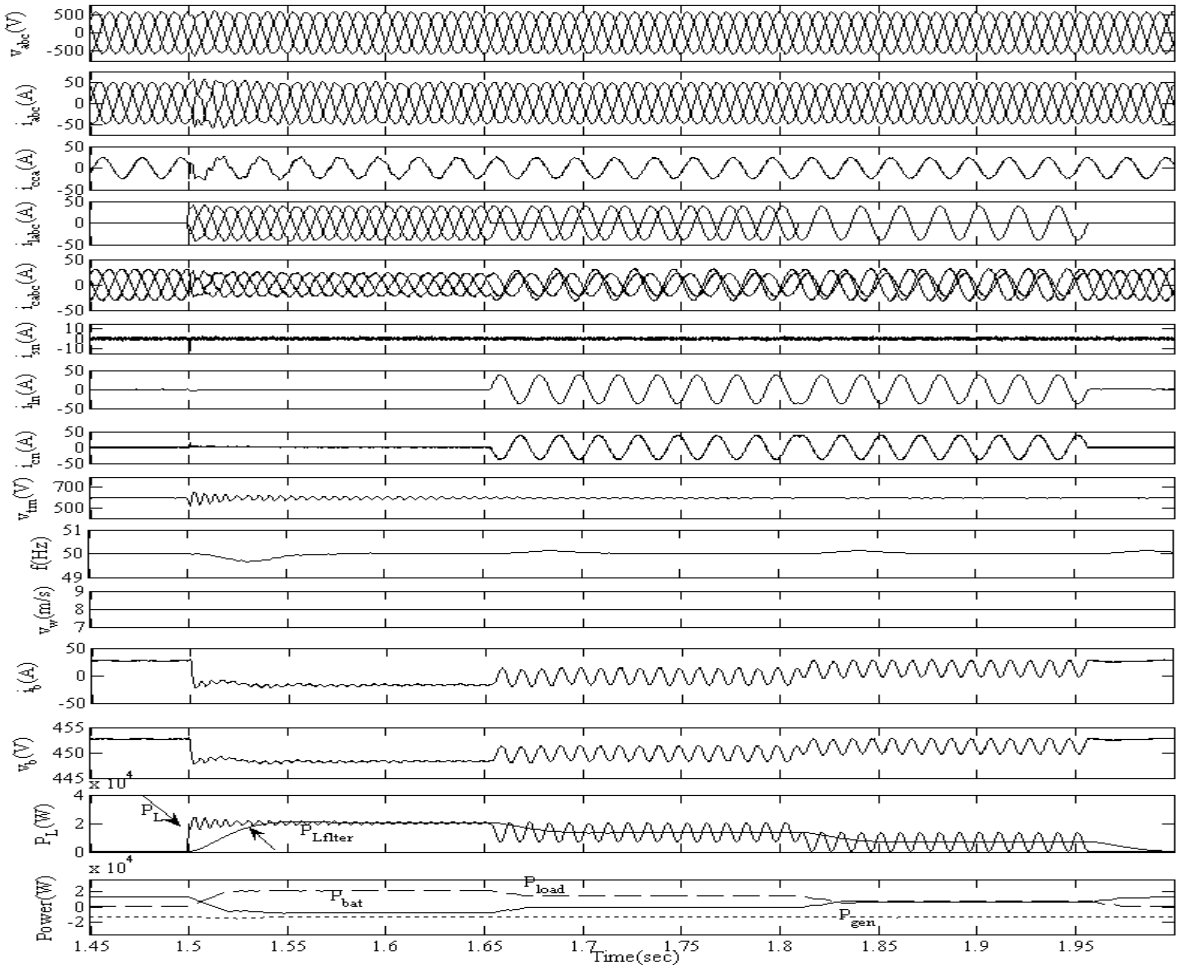

Fig. 4 Transient waveforms during application of balanced/unbalanced linear load at particular wind speed

presents the total harmonic distortions (THD) of the generator voltage and current and under different non-linear load conditions.

6.1 Performance of the controller feeding linear and non-linear loads

Fig 4 demonstrates the performance of the controller with resistive loads at fixed wind speed. At 1.5 sec a three-phase 18kW resistive load is applied and it is observed that the remaining active power is absorbed by the battery to regulate the frequency. At 1.65 sec one phase and later on at 1.8 sec another phase of the load are opened and the load becomes unbalanced but voltage and current at the generator terminals remain balanced which show the load balancing aspects of the controller.

Similarly Fig 5 demonstrates the performance of the controller for feeding non-linear loads. At 1.55 sec a set of 3-single phase diode bridge rectifier based load with L-C filter and resistive element is applied on the system. It is observed that voltage and frequency remain constant as in the case of a linear load and at 1.7 sec one phase of the load is opened and later on at 1.8 sec another phase is opened the load becomes unbalanced but in such type of worst load condition, the controller maintains the balanced voltage and current at the generator terminal. Total harmonic distortion (THD) of generator voltage (V_a)

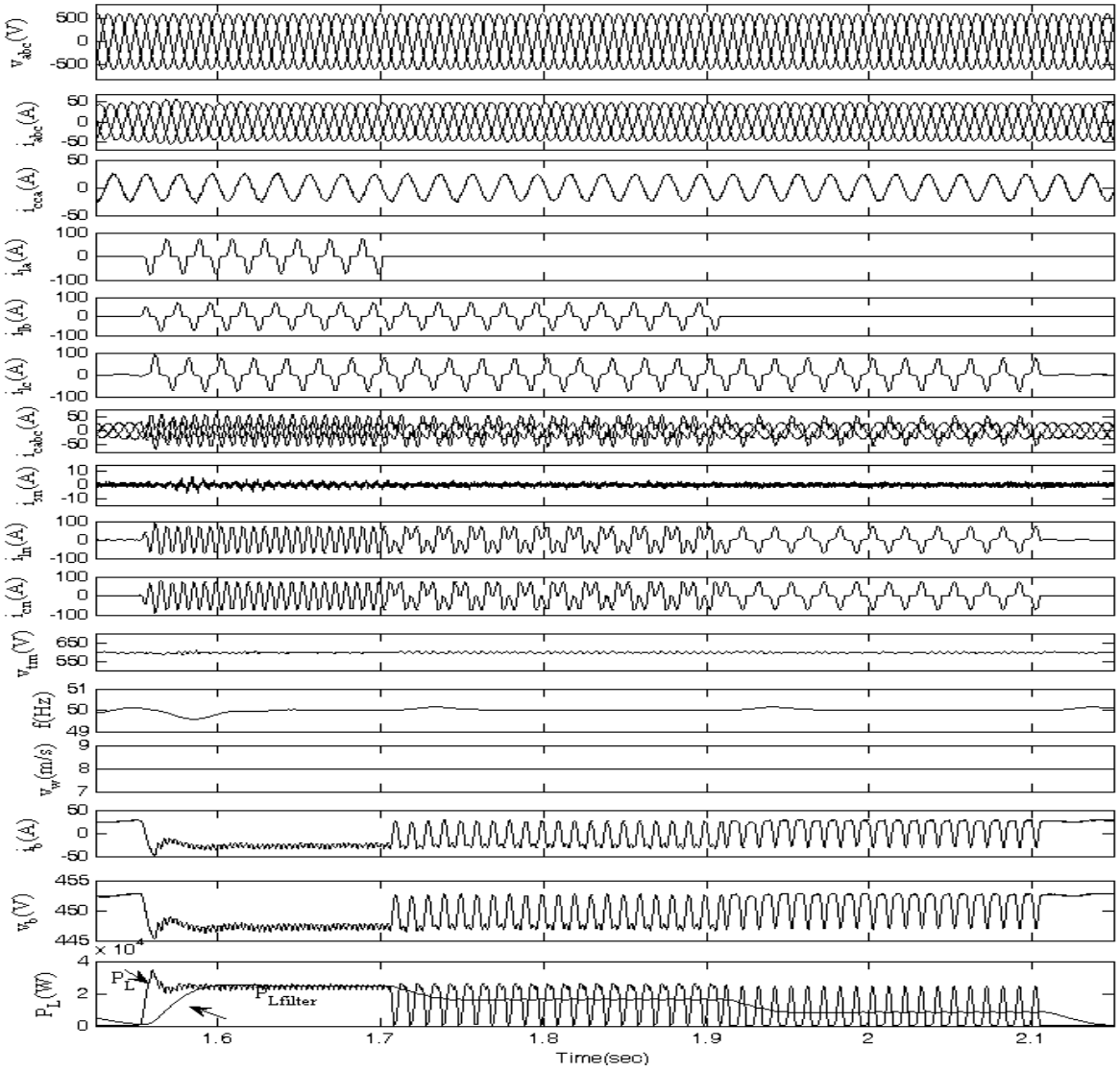

Fig. 5 Transient waveforms during application of balanced/unbalanced non-linear load at particular wind speed

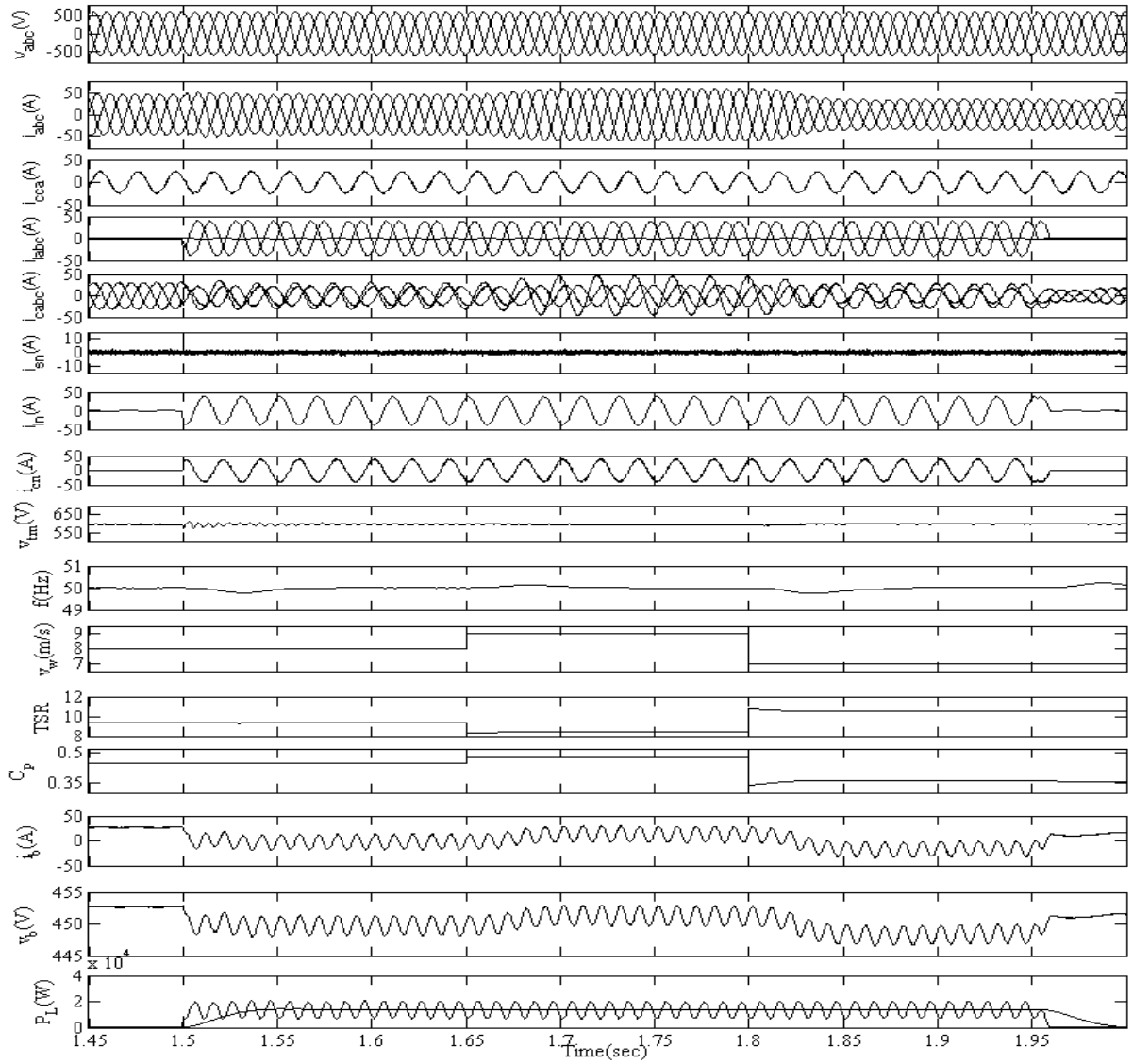

Fig. 6 Transient waveforms during variation of wind speed at particular consumer load

generator current (i_a) and load current (i_{lc}) are given under the condition of balanced and unbalanced non-linear loads (THD) conditions respectively. This is also well within the limit of 5% as per the IEEE-519 standard. In addition to it neutral current of the source, it is also compensated and maintained at zero value.

6.2 Performance of the controller under varying wind speed

Fig. 6 shows the performance of the controller with varying wind speeds at constant applied consumer load. At 1.5 sec when the wind speed is 8m/s, a consumer load (18kW) is applied at the generator terminals. It is observed that due to insufficient power generation at low wind speed, an additional load power is supplied by the battery to regulate the frequency. At 1.65 sec as the wind speed is increased from 8m/s to 9m/s, the generator current (i_{abc}) is increased so that at a particular load, now the current supplied by the battery (i_{bat}) is reduced because now the demand is now met by the generator itself and has the availability of enough wind power. For maintaining the constant speed of the generator for constant frequency operation, it is shown that tip speed ratio (TSR) is also reduced in the same proportion as the wind speed is increased. At 1.8 sec, the wind speed is reduced from 9m/s to 7m/sec then it is observed that the battery again starts discharging

Table 1 Percentage THD OF GENERATOR Voltage, Current, Consumer Load Current At Different Consumer Loads

Non-linear Loads	%THD of generator voltages			%THD of generator currents			% THD of consumer load currents		
	v_a	v_b	v_c	i_a	i_b	i_c	i_{la}	i_{lb}	i_{lc}
Balanced full load (18kW)	.86	.82	.85	2.08	2.18	2.13	45	45.6	45.2
Unbalanced two phase load (12kW)	1.02	1.05	.98	2.2	2.24	2.28	-	48.5	48.8

to meet the demand of the consumer loads. At 1.95 sec when the load is fully removed it is shown that the battery starts charging to store the total generated power. In this manner, the controller provides the load leveling and the control of the frequency. Here an interesting observation is also made that the response of the controller under electrical dynamic conditions (load variation) is faster than the mechanical dynamic conditions (wind speed variation). The frequency regulation under the electrical dynamic condition is also much faster than the mechanical dynamic condition. It is mainly because mechanical time constant is higher than the electrical time constant.

7. Conclusion

The performance of the VF controller has been demonstrated under the conditions of varying balanced/unbalanced linear and non-linear consumer loads as well as under the conditions of varying wind speed. It has been observed that the controller responds in a desired manner and maintains the magnitude and frequency of the generated voltage along with functioning as a harmonic eliminator, a load balancer and a neutral current compensator.

Appendix

The parameters of 22kW, 415V, 50Hz, Y-connected, 4-pole asynchronous machine are given below.

R_s = 0.2511Ω, R_r =0.2489Ω, X_{lr}= X_{ls}= .52Ω, J = 0.304 kg-m^2, C = 12 kVAR

$L_m = 0.075$ $I_m<8.0$

$L_m = 0.075-0.003(I_m-8.0)$ $8<I_m<13$

$L_m = 0.06-0.002(I_m-13)$ $13<I_m<23$

$L_m = 0.041$ $I_m>23$

Battery specification

C_b = 40000F, R_b = 10kΩ, R_s = 0.01Ω, V_{oc} = 450V

Controller parameters

L_f = 3mH, R_f = 0.1Ω, and C_{dc} = 8000μF, N_1:N_2 = 1:1

K_{pa} = 0.18, K_{ia} = 0.01; K_{pf} = 43, K_{if} = 3250.

Wind turbine specification

Rating 22kW, C_{pmax} = 0.48, λ_m = 8.1

C_1= 0.5176, C_2= 116, C_3=0.4, C_4= 5, C_5= 21, C_6= 0.0068, C_7= 0.08, C_8= 0.035.

References

[1] G.K.Singh, "Self-excited induction generator research- a survey," Electric Power Systems Research, vol 69, no. 2-3, pp. 107-114, May 2004.

[2] Jean-Marc Chapallaz, Dos Ghali Peter Eichenberger, Gehard Fischer, "Manual on induction motors used as generators" Deutsches Zentrum Fur Entwicklingstechnologien- GATE 1992.

[3] R.C. Bansal, Ahmed F. Zobba and R.K. Saket, "Some issues related to power generation using wind energy conversion systems: an overview," International Journal of Emerging Electric Power Systems, vol 3, no.2, 2005.

[4] R. K. Verma and T.S. Sidhu, "Bibliographic review of FACTS and HVDC applications in wind power systems," International Journal of Emerging Electric Power Systems, vol 7, no.3, Art7, 2006.

[5] B.Singh, S.S. Murthy and Sushma Gupta, "A voltage and frequency controller for self-excited induction generators" Electrical Power Components and Systems, vol., 34, pp 141-157, 2006.

[6] Juan M. Ramirez and Emmanuel Torres M., "An electronic load controller for self excited induction generators" in IEEE PES General Meeting, June 24-28, 2007, Thampa, FL.

[7] B. Singh, S.S. Murthy and Sushma Gupta, "Analysis and implementation of an electronic load controller for a self excited induction generator" IEE Proc.-Gener. Transm. Distrib., vol. 151, no. 1, pp. 51-60, January 2004.

[8] R. Bonert and S. Rajakaruna, "Self-excited induction generator with excellent voltage and frequency control," IEE Proc.-Gener. Transm. Distrib., vol. 145, no. 1, pp. 33-39, January 1998.

[9] T. Ahmed, O. Noro, K. Matsuo, Y. Shindo and M. Nakaoka, "Wind turbine coupled three-phase self-excited induction generator voltage regulation scheme with static VAR compensator controlled by PI controller" International Journal of Emerging Electric Power Systems, vol 7, no.3, art7, 2006.

[10] S. Wekhande and V. Agrawal, "A new variable speed constant voltage controller for self-excited induction generator," Electric Power System Research, vol. 59, pp. 157-164, 2001.

[11] Luiz A.C. Lopes and Rogerio G. Almeida, "Wind-driven induction generator with voltage and frequency regulated by a reduced rating voltage source inverter", IEEE Trans. on Energy Conversion, vol. 21, no. 2, pp. 297-304, June 2006.

[12] Mohamed S. Elmoursi, Adel M. Sharaf, "Novel STATCOM controllers for voltage stabilization of stand alone hybrid (Wind/small hydro) schemes" International Journal of Emerging Electric Power Systems, vol.7, no.3, Sept 2006.

[13] S. S. Yenga Narayana and V. J. Johnny, "Contributions to the steady state analysis of wind turbine driven induction generator," IEEE Trans. on Energy Conversion, vol. 1, no. 1, pp. 169-175, March 1986.

[14] C. S. Demoulias and P. S. Dokopoulos, "Transient behaviour and self-excitation of wind-driven induction generator after its disconnection from the power grid," IEEE Trans. on Energy Conversion, vol. 5, no. 2, pp. 272-278, June 1990.

[15] E.S. Abdin and W. Xu, "Control design and dynamic performance analysis of a wind turbine –induction generator unit" IEEE Trans. on Energy Conversion, vol. 15, no. 1, pp 91-96, March 2000.

[16] E.S. Abdin, "Digital output controller design for a wind-induction generator conversion scheme," in Proc. of IEEE Industrial Electronic Society Conf, (IECON 2000), vol.2, pp 1439-1444, Oct 2000.

[17] Bhim Singh, Kamal-Al-Haddad and Ambrish Chandra, "A review of active filters for power quality Improvement," IEEE Trans. on Industrial Electronics, vol. 46, no. 5, pp 960-970, Oct. 1999.

[18] M.D. Aderson and D.S Carr., "Battery energy storage technology" IEEE Proc, vol 81, March 1993, pp 475-479.

[19] N. Mohan, T.M. Undeland and W.P. Robbins, "Power Electronics: Converters, Applications and Design," John Willey and Sons, Singapore, Third Edition, 2004.

[20] Siegfried Heier, "Grid Integration of Wind Energy Conversion Systems," John Wiley & Sons Ltd, 1998.

[21] S.N. Bhadra, D. Kastha, and S.Banerjee, "Wind Electrical Systems" 1st Ed. Oxford University Press, New Delhi, 2004.

Bhim Singh (SM'99) was born in Rahamapur, India, in 1956. He received his B.E (Electrical) degree from the University of Roorkee, Roorkee, India, in 1977 and his M.Tech and Ph.D. degree from the Indian Institute of Technology (IIT) Delhi, New Delhi, India, in 1979 and 1983, respectively. In 1983, he joined the Department of Electrical Engineering, University of Roorkee, as a lecturer, and in 1988 became a Reader. In December 1990, he joined the Department of Electrical Engineering, IIT Delhi, as an Assistant Professor. He became an Associate Professor in 1994 and Professor in 1997. His area of interest includes power electronics, electrical machines and drives, active filters, FACTS, HVDC and power quality. Dr. Singh is a fellow of Indian National Academy of Engineering (INAE), the Institution of Engineers (India) (IE (I)), and the Institution of Electronics and Telecommunication Engineers (IETE). He is also a life member of the Indian Society for Technical Education (ISTE), the System Society of India (SSI), and the National Institution of Quality and Reliability (NIQR) as well as a Senior Member of Institute of Electrical and Electronics Engineers (IEEE).

Gaurav Kumar Kasal was born in Bhopal, India, in Nov, 1978. He received his B.E (Electrical) and M.Tech degree from the National Institute of Technology (NIT) Allahabad and National Institute of Technology (NIT) Bhopal, India respectively in 2002 and 2004. Since Dec. 2004, he has been pursuing his Ph. D. degree with the Department of Electrical Engineering, Indian Institute of Technology (IIT) Delhi, New Delhi, India. His field of interests includes power electronics and drives, renewable energy generation and applications, flexible AC transmission system.